

FoCTTA: Low-Memory Continual Test-Time Adaptation with Focus

Youbing Hu¹, Yun Cheng^{2*}, Zimu Zhou³, Anqi Lu¹, Zhiqiang Cao¹, Zhijun Li^{1*}

¹Faculty of Computing, Harbin Institute of Technology

²Swiss Data Science Center, Zurich, Switzerland

³City University of Hong Kong

youbing@stu.hit.edu.cn, yun.cheng@sdsc.ethz.ch, zimuzhou@cityu.edu.hk,

luanqi@stu.hit.edu.cn zhiqiang_cao@stu.hit.edu.cn, lizhijun_oshit.edu.cn

Abstract

Continual adaptation to domain shifts at test time (CTTA) is crucial for enhancing the intelligence of deep learning enabled IoT applications. However, prevailing TTA methods, which typically update all batch normalization (BN) layers, exhibit two memory inefficiencies. First, the reliance on BN layers for adaptation necessitates large batch sizes, leading to high memory usage. Second, updating all BN layers requires storing the activations of all BN layers for backpropagation, exacerbating the memory demand. Both factors lead to substantial memory costs, making existing solutions impractical for IoT devices. In this paper, we present FoCTTA, a low-memory CTTA strategy. The key is to automatically identify and adapt a few drift-sensitive representation layers, rather than blindly update all BN layers. The shift from BN to representation layers eliminates the need for large batch sizes. Also, by updating adaptation-critical layers only, FoCTTA avoids storing excessive activations. This focused adaptation approach ensures that FoCTTA is not only memory-efficient but also maintains effective adaptation. Evaluations show that FoCTTA improves the adaptation accuracy over the state-of-the-arts by 4.5%, 4.9%, and 14.8% on CIFAR10-C, CIFAR100-C, and ImageNet-C under the same memory constraints. Across various batch sizes, FoCTTA reduces the memory usage by 3-fold on average, while improving the accuracy by 8.1%, 3.6%, and 0.2%, respectively, on the three datasets.

Introduction

After deploying deep neural networks (DNNs) to IoT devices for real-world applications, the model accuracy often severely degrades when there is a notable shift between the source and the target domain (Liang, Hu, and Feng 2020; Liu et al. 2021; Ma et al. 2023; Montesuma, Mboula, and Souloumiac 2023). In such cases, the pre-trained model should adapt to the target data distribution at test time without access to the target data labels, known as *Test-Time Adaptation* (TTA) (Wang et al. 2020). As the target domain may evolve over time, continual test-time adaptation (CTTA) (Wang et al. 2022) is necessary, and has attracted increasing research interest (Chen et al. 2024; Park et al. 2024; Gao, Zhang, and Liu 2024; Wang et al. 2024).

As a continual unsupervised domain adaptation paradigm for IoT applications, CTTA must consider not only *effec-*

tiveness (e.g., accuracy), but also *efficiency* (e.g., computation, memory, latency) when it comes to *what*, *when*, and *how* to adapt. Due to the unsupervised nature, TTA solutions (Wang et al. 2020; Niu et al. 2023) often minimize an entropy-based loss by updating certain model parameters via standard mini-batch gradient descent. The adaption can be performed upon all test-time samples or selectively to reliable samples. For example, EATA (Niu et al. 2022) selects reliable samples through entropy filtering for each predicted sample. Most CTTA methods adopt a *partial training* strategy, which only updates a small set of model parameters at test-time, for both effective adaptation and computation efficiency (Boudiaf et al. 2022; Park et al. 2024).

Although mainstream CTTA proposals (Niu et al. 2022; Yuan, Xie, and Li 2023; Niu et al. 2023; Gong et al. 2023) opt for *computation* efficiency, it does not easily translate into *memory* efficiency, which is crucial for IoT applications. Specifically, they update the affine parameters of all batch normalization (BN) layers to adapt to the target domain. Even though a small set of parameters are updated, this strategy demands substantial memory to function properly. (i) A large batch size is necessary to accurately estimate the current batch statistics. (ii) Updating the BN layers still involves storing activations for backpropagation, whose memory cost increases with the number of BN layers updated. Both factors lead to considerable memory overhead to maintain high adaptation accuracy. Fig. 1(a) shows the memory usage of TENT (Wang et al. 2020), the earliest TTA method, with the increase of batch size. As shown in Fig. 1(b), the BN-based method is sensitive to the batch size. In the target domain, it can only retain accuracy higher than the original pre-trained model (36.5MB) by consuming $8\times$ memory.

A few pioneer CTTA schemes have been proposed to improve memory efficiency (Hong et al. 2023; Song et al. 2023) (see Table 1). Compared with standard methods that update all affine parameters in all BN layers (Wang et al. 2020; Niu et al. 2022), these solutions either update shift-sensitive channels in the BN layers (Hong et al. 2023; Lim et al. 2022), or completely freeze the original model and only update extra side-way prompt modules (Song et al. 2023; Gan et al. 2023). These schemes improve memory efficiency by reducing the number of adapted layers (channels), which saves the storage of activations during backpropagation. However, they still rely on large batch sizes to

*Corresponding Author

Table 1: **Comparing our approach and associated CTTA adaptation settings for memory efficiency.** Our method only optimizes the adaptation-critical representation layer, eliminating the need for large batch sizes and avoiding the storage of numerous activations.

Optimization parameters	Batch Size	Intermediate Activation
Parameters of all BN layers (Wang et al. 2020)	Large	Large
Parameters of specific BN layers (Hong et al. 2023)	Large	Smaller
Additional prompt modules (Song et al. 2023)	Large	Smaller
Adaptation-critical representation layers (Ours)	Smaller	Smaller

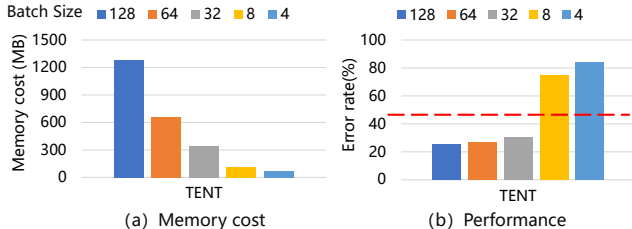


Figure 1: Evaluate TENT memory cost and performance across various batch sizes. (a) TENT memory costs at different batch sizes. (b) TENT performance at different batch sizes. The red dashed line represents the performance of the pre-trained model, i.e., without using any CTTA method.

boost adaptation accuracy, making them still sub-optimal for low-memory adaptation.

In this paper, we aim at memory-efficient CTTA that functions with small batch sizes and low activation storage during backpropagation. Specifically, we choose to update the representation layers rather than the BN layers to be more resilient to batch sizes. In addition, observing the importance of representation layers varies for adaptation, we only update the top-K critical representation layers to reduce the storage of activations. By *focusing on adaptation-critical representation layers*, we not only ensure memory efficiency but also achieve high adaptation accuracy. This is implemented via an offline warm-up training stage after pre-training but before testing, where simulated unseen distribution shifts are used to identify shift-sensitive representation layers via a simple gradient-based importance metric. At test time, only the top-K critical representation layers are updated for adaptation. Experimental results show that our approach achieves state-of-the-art performance on standard benchmarks. Our main contributions are summarized as follows.

- We leverage the representation layers rather than the BN layers in the pre-trained model for CTTA. This paradigm shift mitigates the reliance on large batch size, an obstacle towards memory-efficient CTTA.
- We empirically show that the importance of representation layers differs for TTA, and propose a simple metric to identify adaptation-critical representation layers. The layer-wise selective updating scheme notably reduces the storage of activations for TTA.
- We extensively validate the effectiveness of our solution on various models and datasets. Under the same mem-

ory constraints, we outperform the state-of-the-art CTTA methods SAR, ECoTTA, and EATA, showing accuracy improvements of 4.5%, 4.9%, and 14.8% on CIFAR10-C, CIFAR100-C, and ImageNet-C, respectively. Notably, we achieve a threefold reduction in average memory usage across different batch sizes, while boosting average accuracy by 8.1%, 3.6%, and 0.2% on the three datasets.

Related Work

Test-Time Adaptation

Test-time adaptation (TTA) addresses shifts between source and target domains during testing without accessing source data (Wang et al. 2020; Lee et al. 2023; Niu et al. 2023; Park et al. 2024). For example, TENT (You, Li, and Zhao 2021) proposes an entropy minimization based unsupervised test-time objective, and adapts to the target domain by updating the affine transformations in the BN layers. Alternatively, SHOT (Liang, Hu, and Feng 2020) considers adaptation as source hypothesis transfer, and updates the feature representation layers to the target domain while keeping the classification layers unchanged. As an orthogonal solution, EATA (Niu et al. 2022) only selects reliable samples for adaptation. Continual TTA (CTTA) (Wang et al. 2022) extends the scope of TTA from a single target domain to a sequence of continuously changing domains. SWA (Yang et al. 2023) explores safety supervision for CTTA. SAR (Niu et al. 2023) proposes a sharpness-aware and reliable entropy minimization to stabilize CTTA. LAW (Park et al. 2024) leverages Fisher Information Matrix (FIM) to identify layers to keep or adapt.

Among the questions of *what*, *when*, and *how* to adapt in CTTA, we focus on *what* to update at low *memory* cost, and adopt standard approaches for the other two issues, i.e., entropy-based sample selection (Niu et al. 2022) and entropy minimization-based loss (You, Li, and Zhao 2021).

Efficient On-device Model Adaptation

There is an increasing interest to enable model adaptation on memory-limited platforms (Lin et al. 2020), where the bottleneck lies in the storage of activations and the use of large batch size for effective backpropagation (Cai et al. 2020). As a special model adaptation problem (unsupervised continual domain adaptation), CTTA faces the same memory bottleneck, and a few pioneer studies have explored memory-efficient CTTA. For example, TENT (Wang et al. 2020) reduces activation during adaptation by exclusively updating BN layers. MECTA (Hong et al. 2023) further prunes activations of cached BN layers during backpropagation. EcoTTA

(Song et al. 2023) keeps the entire model parameters frozen and only updates a small set of extra meta layers. Although these approaches significantly reduce the memory consumption by saving storage of activations, they still depend on large batch sizes. To operate with small batch sizes, SAR (Niu et al. 2023) replaces the BN with layer normalization (group normalization). TTN (Lim et al. 2022) adjusts the weight of the BN layers updated by the test-time batch according to the domain offset sensitivity of each BN layer.

Unlike the solutions above, we target at memory-efficient CTТА with both reduced activation size and batch size. The key idea is to update only a few representation layers sensitive to distribution shifts.

Problem Statement

Continual TТА We consider the standard continual test-time adaptation (CTТА) setup (Wang et al. 2020; Liang, Hu, and Feng 2020; Wang et al. 2022). A model $f_{\theta}(y|x)$ with parameters θ is pre-trained on source data $D_s = (X^S, Y^S) = \{(x, y) \sim p_s(x, y)\}$, where $x \in X^S$ is e.g., an image and $y \in Y^S$ is its associated label from the source class set Y^S . The target data are *unlabeled* and sampled from an arbitrary target distribution $D_t = \{x \sim p_t(x)\}$, where $p_t(x)$ undergoes *continual* changes over time t . Following the covariate shift assumption (Storkey et al. 2009), $p_s(y|x) = p_t(y|x)$ and $p_s(x) \neq p_t(x)$. As the target distribution gradually shifts from the source, $f_{\theta}(y|x)$ no longer approximates $p(y|x)$, and needs adaptation to retain accuracy. Unique in CTТА, θ_t should make predictions online when source data is absent and adapt themselves into θ_{t+1} for the subsequent input, given access to only $p_t(x)$ at time step t .

Memory Footprint of CTТА In CTТА, the model f_{θ} is often a neural network $f_{\theta}(\cdot) = f_{\theta_L}(f_{\theta_{L-1}}(\dots(f_{\theta_1}(\cdot))\dots))$, with parameters θ_l in layer l . Assume the parameter θ_l consists of weights W_l and bias b_l , and the input and output features of this layer are a_l and a_{l+1} , respectively. Given the forward pass $a_{l+1} = a_l W_l + b_l$, the corresponding backward pass with batch size 1 is

$$\frac{\partial \mathcal{L}}{\partial a_l} = \frac{\partial \mathcal{L}}{\partial a_{l+1}} W_l^T, \frac{\partial \mathcal{L}}{\partial W_l} = a_l^T \frac{\partial \mathcal{L}}{\partial a_{l+1}}, \frac{\partial \mathcal{L}}{\partial b_l} = \frac{\partial \mathcal{L}}{\partial a_{l+1}} \quad (1)$$

Eq. 1 shows that to update a learnable layer with weight W_l , one must store all a_l to compute the gradients. Hence, for a model with L layers, the memory cost during backpropagation given batch size B can be estimated as

$$m(cost) = \sum_{l=1}^L (m(\theta_l) + m(a_l) \cdot B) \quad (2)$$

where $m(\cdot)$ denotes the memory requirements. From Eq. 2, the memory cost of adaptation (via gradient descent) increases with # layers L updated and the batch size B . Note that memory of the weights θ are constant during adaptation.

Parameters to Update in CTТА Existing CTТА methods update the pre-trained model $f_{\theta}(y|x)$ at test-time to better approximate $p(y|x)$. The parameters θ are often divided

into adaptable weights θ^a and frozen weights θ^f , where the adaptable weights are updated by minimizing an unsupervised loss $\mathcal{L}(x; \theta^a \cup \theta^f), x \sim p_t(x)$ w.r.t. θ^a (Boudiaf et al. 2022). CTТА methods differ in their choices of the parameter partition $\{\theta^a, \theta^f\}$ and loss function \mathcal{L} , where the choice of adaptable weights θ^a affects the memory cost. Most CTТА proposals opt for *computation efficiency*, which does not translate into *memory efficiency* due to the storage of substantial activations and the use of large batch sizes. Therefore, we focus on identifying adaptable weights θ^a that yield low memory cost without compromising adaptation accuracy.

Method

We propose FoCTТА, a memory-efficient CTТА scheme that focuses on adaptation-critical representation layers. FoCTТА updates representation layers rather than BN layers to mitigate dependence on a large batch size B . It also selectively updates the representation layers to reduce the number of adaptable layers L . From Eq. 2, the reduction of B and L decreases the memory usage during mini-batch gradient descent, the key memory bottleneck in CTТА. Fig. 3 illustrates the workflow of FoCTТА.

Updating Representation Layers for CTТА

As mentioned, a core issue in CTТА is to decide the adaptable parameters θ^a . Inspired by the concept of source hypothesis transfer (Liang, Hu, and Feng 2020), we focus on representation layers for CTТА. According to (Liang, Hu, and Feng 2020), $f_{\theta}(y|x)$ can be decomposed into a feature extractor g_s and a classifier h_s , where $f_{\theta}(y|x) = h_s(g_s(y|x))$. It suffices to update g_s for CTТА. Since adapting the feature extractor reduces the number of adaptable layers, it holds potential for memory-efficient CTТА. Furthermore, as shown in , updating the representation layers works with small batch sizes, an essential advantage over BN layers.

We push the idea one step forward by asking the following: can we achieve high CTТА accuracy by *selectively* updating the representation layers? That is, we hypothesize that the *importance* of representation layers varies for CTТА, thereby only the critical ones needs updating. Although layer importance and layer-wise fine-tuning have been extensively explored in network pruning (Li et al. 2016; Liu et al. 2017; Lee, Ajanthan, and Torr 2018; Cheng, Zhang, and Shi 2023), their observations were intended for supervised learning in the same domain. It is unclear whether similar observations and hypothesis hold for unsupervised adaptation to domains with shifts.

To this end, we conduct an empirical study to understand the importance of individual representation layers to CTТА. Specifically, we pick three layer importance metrics: gradient norm (Molchanov et al. 2016; Lee, Ajanthan, and Torr 2018), ℓ_1 norm (Liu et al. 2017; Han et al. 2015), and weight norm (Li et al. 2016) commonly used for supervised training without domain shift, and select the top- K important layers ($K = 5$) for adaptation. We tested various models and datasets in standard CTТА benchmarks. Fig. 2 shows the results. More experimental details and results are shown in the

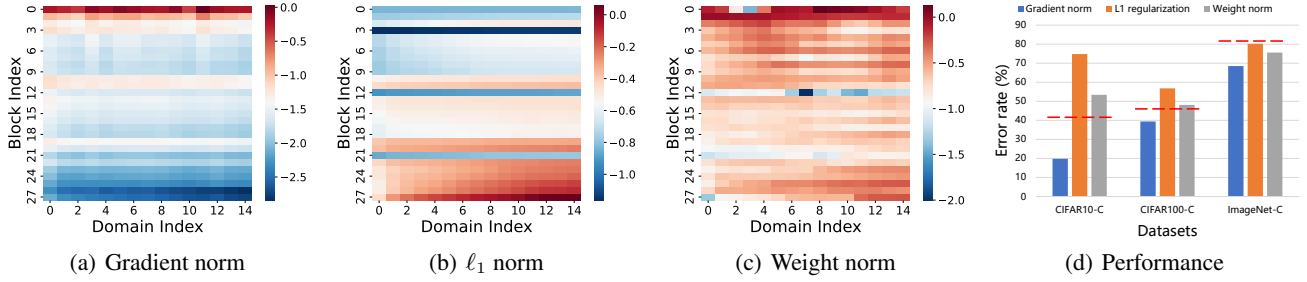


Figure 2: We evaluated the performance of selecting the top-K layers of the adaptation model using various metrics on three commonly used CTTA benchmarks. In addition, we also showcased the feature representation of CTTA during adaptation using various metrics on CIFAR10-C with WideResNet-28. All these results are on a logarithmic scale, and we normalized them by linear transformation with the maximum value set to 0. A larger block index corresponds to deeper layers. (a): Gradient norm of different blocks. (b): ℓ_1 norm of different blocks. (c): Weight norm of different blocks. (d): We optimized the top-K layers of the adaptation model on diverse datasets using varied metrics to assess its performance while keeping the other layers frozen. The red dashed line indicates the performance of the original model.

supplementary material Sec. A. We make the following observations.

- *Importance of representation layers differs for CTTA.* The importance indicated by different metrics varies across layers. For instance, the gradient norm suggests important representation layers are the shallow layers, the ℓ_1 norm shows deeper layers are more important, while the weight norm indicates the critical representation layers are distributed throughout the model.
- *Gradient norm indicates layer importance for CTTA.* Across three datasets, we consistently observe that important representation layers selected by the gradient norm achieve the highest accuracy. The important layers identified by the other two metrics even yield performance lower than the model without adaptation.

These observations validate the hypothesis that layer importance also varies in the context of CTTA and show the gradient norm as an effective importance metric for CTTA.

Identifying Critical Representation Layers

To identify important representation layers sensitive to domain shifts, we leverage an additional *warm-up training* phase after pre-training but before testing. It simulates domain shifts by augmenting the original training data.

Specifically, we take each original data point x and create an augmented counterpart x' that shares the same semantic information. As shown in Fig. 3, in the warm-up training phase, we freeze the classifier h_s of the pre-trained model, optimize the feature extractor g_s with cross-entropy loss using the augmented data x' as input, and collect the gradient norms of each layer of g_s in each batch¹.

The average gradient norm of each layer quantifies the

¹The warm-up phase shows robustness to different data augmentation types, as indicated by the ablation study results in Table 10.

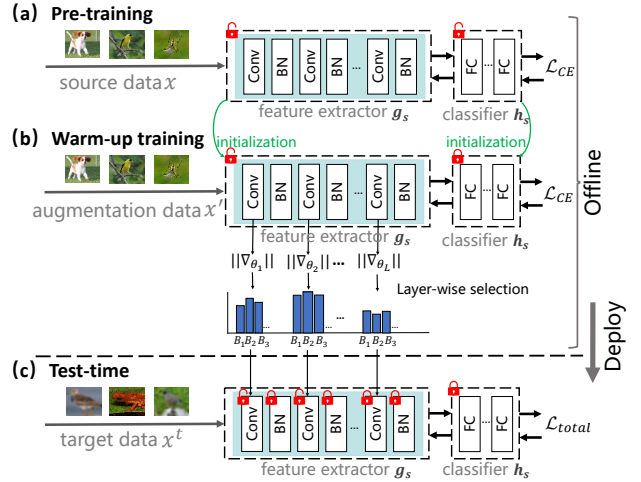


Figure 3: The pipeline of our FoCTTA framework. (a) Pre-training, which is agnostic to architecture and pre-training methods, any pre-trained model can be used as initialization. (b) Warm-up training, which employs augmented data x' of the source data to simulate distributional shifts, computing the sensitivity of each layer in the feature extractor g_s to domain shifts. (c) At test-time t , continuously changing target data x^t is used as input, and only the adaptation-critical representation layer is optimized.

layer’s importance:

$$s = \left[\log \frac{1}{B_N} \sum_{b=1}^{B_N} \|\nabla_{\theta_l}\| \right]_{l=1}^L \quad (3)$$

where B_N , θ_l and ∇_{θ_l} are the N -th batch size, parameters of layer l , gradients of layer l , respectively. The vector s of length L stores the importance of all layers in the pre-trained model. We then sort s from high to low. The layers with the largest average gradient norms are identified as important for CTTA. In practice, the selection is conducted by $\alpha \|s\|$,

where α is a tunable hyperparameter to balance memory cost and accuracy. Note that the warm-up training is performed before test time, which is common in other CTTA solutions (Choi et al. 2022; Jung et al. 2023; Lim et al. 2023; Niu et al. 2022; Song et al. 2023). Also, it does not require access to the source dataset (X^S, Y^S) during test-time, and is agnostic to the architecture and pre-training method of the original model.

CTTA Objective

During test-time adaptation, FoCTTA exclusively optimizes adaptation-crucial layers for the target domains, maintaining the other layers unchanged. In line with (Niu et al. 2022), we utilize the entropy predicted by the adaptation model to identify reliable samples for subsequent model optimization. Consequently, the online adaptation loss function is formulated as

$$\mathcal{L}_{ent} = \mathbb{I}_{\{H(\hat{y}) < H_0\}} \cdot H(\hat{y}) \quad (4)$$

$$H(\hat{y}) = - \sum_c p(\hat{y}) \log p(\hat{y}) \quad (5)$$

where \hat{y} is the prediction output of a test image, and $p(\cdot)$ denotes the softmax function. The symbol $\mathbb{I}_{\{\cdot\}}$ represents an indicator function, and H_0 is a predefined hyperparameter.

In addition, to prevent catastrophic forgetting (Niu et al. 2022; Wang et al. 2022) and error accumulation (Tarvainen and Valpola 2017; Arazo et al. 2020) due to long-term continuous adaptation, we add a regularization term to the loss function when optimizing Eq. 4. The final loss function is formulated as

$$\mathcal{L}_{total} = \mathcal{L}_{ent} + \lambda \sum_{m=1}^M \|\tilde{x}_m - x_m\|_1 \quad (6)$$

where λ is a positive scalar to control the ratio between two terms in the loss function. $M = \alpha \|s\|$ denotes the number of layers to be updated. The terms \tilde{x}_m and x_m represent the m -th output of the adapted model and the original model, respectively. Our evaluations show that a small portion of (1.0%) representation layers need to be updated.

Experiments

Experimental Setup

Datasets. We use CIFAR10, CIFAR100 (Krizhevsky 2009), and ImageNet (Deng et al. 2009) as the source domain datasets, while CIFAR10-C, CIFAR100-C, and ImageNet-C serve as the corresponding target domain datasets. These target domain datasets were originally designed to evaluate the robustness of classification networks (Hendrycks and Dietterich 2019). Each target domain dataset contains 15 types of corruption with 5 severity levels. Following (Wang et al. 2022), for each corruption, we use 10,000 images for both the CIFAR10-C and CIFAR100-C datasets, and 5,000 images for the ImageNet-C dataset.

Implementation Detail. All experiments are performed using the PyTorch framework (Paszke et al. 2019). To ensure fair comparisons, we employ identical pre-trained models,

specifically the WideResNet-28 and WideResNet-40 models (Zagoruyko and Komodakis 2016) sourced from RobustBench (Croce et al. 2020), as well as the ResNet-50 (He et al. 2016) model from TTT++ (Liu et al. 2021). During the warm-up training phase, data augmentation techniques such as color jittering, padding, random affine, center cropping, invert, and random horizontal flipping were applied to all source data. Subsequently, the pre-trained model is fine-tuned for one epoch using cross-entropy loss and the Adam optimizer with a learning rate of 0.00025 to identify adaptation-crucial layers. At test-time, similar to (Wang et al. 2022), we employ the Adam optimizer with a learning rate of 0.001 for the CIFAR datasets, while for ImageNet, a learning rate of 0.00025 is utilized. In Eq. (4), the entropy threshold H_0 is set to $0.4 \times \ln C$, where C denotes the number of task classes. We empirically set $\lambda = 1$ and $\alpha = 0.1$.

Evaluation setup. We assess the effectiveness and memory efficiency of various methods through two configurations: 1) **Under memory constraints**, we test the error rates for each method. 2) **Under the same batch size**, we compute the error rates and memory consumption for each method, including the model parameters and the activation size. We demonstrate the memory efficiency of our work by using the official code provided by TinyTL (Cai et al. 2020).

Baselines. We compare our method with several state-of-the-art continual test-time adaptation algorithms, includes Source, Continual TENT (Wang et al. 2020), CoTTA (Wang et al. 2022), ECoTTA (Song et al. 2023), EATA (Niu et al. 2022), SAR (Niu et al. 2023), SWA (Yang et al. 2023), and LAW (Park et al. 2024). All methods cannot access additional data in any way; i.e., these methods cannot be reset to the initial pre-trained model.

Performance Evaluation

Performance with memory constraints. Evaluating accuracy under memory constraints by adjusting batch sizes to achieve comparable memory consumption among all methods. Table 2 presents per-domain error rates in CTTA, organized by columns, along with average memory consumption and error rate. Analyzing Table 2, we find that FoCTTA significantly improves accuracy in memory-constrained settings across all datasets and models. Adapting all BN layer affine parameters (TENT, EATA, SAR) or all model parameters (CoTTA, SWA, LAW) requires storing a considerable amount of activations for backpropagation. This compels them to use smaller batch sizes to meet memory constraints, leading to significant performance degradation and even collapse. For example, when the memory constraint is 50MB, TENT achieves 87% performance on CIFAR100-C, while the original model’s performance is 46.8%. Compared to ECoTTA, which requires updating additional side-way meta networks to adapt to the target domain, our FoCTTA only needs updates for 1.0% of the representation layers. As a result, it achieves an average accuracy improvement of 14.8% across three datasets compared to ECoTTA. Across all models and datasets, FoCTTA outperforms these state-of-the-art approaches SAR, ECoTTA, and EATA, showing significant accuracy improvements of 4.5%, 4.9%, and 14.8% on CIFAR10-C, CIFAR100-C, and ImageNet-C, respectively.

Table 2: **Comparison of error rate (%) on the highest corruption severity under memory constraints.** We conduct experiments on CTTA setup. CIFAR10-C uses WideResNet-28, CIFAR100-C employs WideResNet-40, and ImageNet-C utilizes ResNet-50. Avg. err means the average error rate (%) of all 15 corruptions, and Mem. denotes total memory consumption, including model parameter sizes and activations. The lowest error is in bold, and the second lowest error is underlined.

Datasets	Method	t →															Avg. err	Mem.
		Gaus.	Shot	Impu.	Defo.	Glas.	Moti.	Zoom	Snow	Fros.	Fog	Brig.	Cont.	Elas.	Pixe.	Jpeg		
CIFAR10-C	EATA	<u>24.5</u>	20.2	<u>30.2</u>	16.2	<u>32.9</u>	19.9	16.9	22.1	22.4	19.2	13.7	19.6	27.9	22.6	26.4	22.3	394.0
	Continual TENT	25.1	22.8	35.4	21.9	40.3	30.8	25.5	30.1	34.2	38.1	31.9	42.6	44.7	40.0	46.6	34.0	394.0
	CoTTA	99.8	99.8	99.8	99.8	99.8	99.8	99.8	99.8	99.8	99.8	99.8	99.8	99.8	99.8	99.8	99.9	394.2
	SWA	99.8	99.8	99.8	99.8	99.8	99.8	99.8	99.8	99.8	99.8	99.8	99.8	99.8	99.8	99.8	99.9	394.2
	ECoTTA	27.8	22.8	31.3	16.1	34.6	17.8	15.4	19.9	18.7	17.6	12.1	16.5	27.1	22.2	27.6	21.8	397.0
	SAR	29.0	26.9	35.7	<u>13.5</u>	35.4	<u>14.9</u>	<u>13.1</u>	<u>18.4</u>	<u>18.2</u>	<u>15.8</u>	<u>9.2</u>	<u>13.7</u>	<u>24.6</u>	<u>20.6</u>	28.8	<u>21.2</u>	394.0
	LAW	26.6	23.8	31.2	22.0	35.1	24.6	20.3	23.4	21.9	22.0	16.6	19.1	27.2	22.8	24.6	24.1	378.8
	FoCTTA (Ours)	22.4	<u>21.1</u>	25.5	11.8	29.0	13.1	10.3	15.4	15.1	12.3	7.6	10.9	20.9	15.2	19.8	16.7	356.0
CIFAR100-C	EATA	45.4	43.5	47.0	39.8	50.6	41.8	39.9	44.1	44.0	45.7	38.3	40.8	47.1	43.0	50.3	44.1	47.9
	Continual TENT	45.0	48.3	64.4	78.5	95.4	96.5	96.7	96.9	97.4	97.6	97.6	98.0	97.9	97.7	97.9	87.0	47.9
	CoTTA	64.7	72.6	80.9	85.1	91.7	94.2	96.4	97.2	97.3	97.9	97.7	98.2	98.2	98.3	98.4	91.3	50.7
	SWA	62.3	71.8	79.8	83.6	82.5	93.7	96.2	97.1	97.3	98.0	97.6	97.7	98.0	98.1	98.4	90.1	50.7
	ECoTTA	<u>44.9</u>	<u>41.2</u>	<u>44.9</u>	<u>34.8</u>	<u>45.5</u>	<u>35.4</u>	<u>33.4</u>	<u>38.5</u>	<u>38.4</u>	<u>41.8</u>	<u>33.0</u>	<u>38.9</u>	<u>41.3</u>	<u>36.3</u>	<u>45.8</u>	<u>39.6</u>	<u>45.8</u>
	SAR	45.5	44.9	49.5	44.2	56.4	52.5	52.1	62.2	67.9	80.3	86.7	96.5	96.8	97.2	97.2	68.7	47.9
	LAW	61.7	68.4	83.8	91.2	96.7	97.3	97.7	97.8	98.0	97.9	97.8	98.1	98.0	98.0	98.0	92.0	46.1
	FoCTTA (Ours)	39.3	38.9	37.5	29.9	40.3	31.6	30.0	34.6	33.5	37.7	27.2	32.1	36.6	31.8	39.5	34.7	45.9
ImageNet-C	EATA	92.7	91.3	91.9	92.9	93.0	85.5	77.2	76.5	78.6	67.0	51.5	88.4	71.8	66.8	73.6	79.9	385.4
	Continual TENT	85.1	86.8	94.6	99.1	99.5	99.6	99.6	99.5	99.6	99.6	99.5	99.7	99.6	99.6	99.6	97.4	385.4
	CoTTA	96.0	99.6	100.0	100.0	100.0	100.0	100.0	100.0	100.0	100.0	100.0	100.0	100.0	100.0	100.0	99.7	393.8
	SWA	94.3	99.8	100.0	100.0	100.0	100.0	100.0	100.0	100.0	100.0	100.0	100.0	100.0	100.0	100.0	99.6	393.8
	ECoTTA	94.8	97.9	100.0	100.0	99.9	100.0	99.9	100.0	100.0	99.9	100.0	100.0	100.0	99.9	100.0	99.5	427.2
	SAR	92.6	91.4	92.0	93.1	<u>93.0</u>	85.5	79.2	79.1	80.5	70.1	<u>51.3</u>	<u>86.9</u>	<u>71.3</u>	67.6	<u>73.0</u>	80.4	385.4
	LAW	90.7	96.6	99.6	99.8	99.8	99.7	99.7	99.8	99.8	99.7	99.8	99.8	99.8	99.8	99.8	98.9	452.7
	FoCTTA (Ours)	84.1	78.7	79.3	82.1	79.3	69.4	58.4	63.0	64.6	50.4	36.1	77.0	54.8	47.3	47.3	65.1	423.0

Table 3: **Ablation experiments on CIFAR100-C with a batch size of 32.** “Reg.” refers to regularization, and “LS.” denotes layer selection.

Time	Method	t →															Avg. err
		Gaus.	Shot	Impu.	Defo.	Glas.	Moti.	Zoom	Snow	Fros.	Fog	Brig.	Cont.	Elas.	Pixe.	Jpeg	
	FoCTTA	40.4	39.8	38.7	31.4	41.6	32.6	31.5	34.8	34.9	38.3	28.4	33.7	38.2	32.7	40.2	35.8
	w/o Reg.	40.5	40.3	41.5	32.6	41.6	32.6	31.7	34.8	35.2	37.1	28.9	33.6	38.3	33.5	39.8	36.1
	w/o LS.	99.0	99.0	99.1	99.0	99.0	95.8	99.0	98.9	99.0	98.8	99.0	99.0	99.0	98.7	99.0	98.7
	w/o Reg. and LS.	98.6	99.0	99.0	99.0	98.4	97.1	98.6	99.1	98.7	99.2	98.4	98.7	99.1	98.8	99.0	98.7

With these findings, we emphasize FoCTTA’s superiority in resource-constrained environments. It automatically identifies and adapts a few drift-sensitive representation layers, rather than blindly updating all BN layers. The shift from BN to representation layers eliminates the need for large batch sizes. Also, by updating adaptation-critical layers only, FoCoTTA avoids storing excessive activations. This achieves simultaneous optimization of memory efficiency for CTTA adaptation in both batch size and activation. Additionally, we uncover challenges faced by full-parameter update methods under memory constraints, particularly performance collapse with smaller batch sizes. This research enhances understanding of different methods’ adaptability and performance in memory-constrained environments.

Performance with the same batch size. Table 4 presents the online measurement average error rate and memory consumption on the corrupted dataset under CTTA, considering different batch sizes, models, and datasets. Clearly, FoCTTA achieves a threefold reduction in average memory consumption while improving average accuracy by 8.1%, 3.6%, and 0.2% on CIFAR-10C, CIFAR-100C, and ImageNet-C, respectively. This demonstrates that FoCTTA maintains robustness across a wide range of batch sizes while remaining memory-efficient. The superior performance of FoCTTA,

from its strategy of updating the adaptation-critical representation layers during adaptation, only mitigates its reliance on batch size. Unlike methods that optimize all BN layers (TENT, EATA, SAR), which rely on larger batch sizes. While methods that update all parameters (CoTTA, SWA, LAW) need to store a large number of activations. FoCTTA optimizes CTTA from both batch size and activation. Therefore, FoCTTA can provide significant memory savings without compromising accuracy.

Adaptation time. Table 6 presents the average adaptation times across various methods for each domain. These measurements were obtained through testing on the CIFAR10-C dataset using a single NVIDIA 3090 GPU, employing the WideResNet-28 model with a batch size of 32. Also, we show their average error rates overall of 15 corruptions. From Table. 6, it is clear that FoCTTA significantly reduces adaptation time with optimal performance compared to state-of-the-art CTTA methods. Specifically, compared to CoTTA, FoCTTA reduces adaptation time by a factor of 113, while compared to the fastest adaptation method EATA, FoCTTA improves adaptation time by a factor of 2. This advantage primarily results from (i) updating only a few adaptation-critical representation layers, effectively reducing computation during backpropagation, and (ii) selecting

Table 4: **Comparison of error rate (%) and memory consumption (MB) on the highest corruption severity under the same batch size.** We conduct experiments on CTTA setup. CIFAR10-C uses WideResNet-28, CIFAR100-C employs WideResNet-40, and ImageNet-C utilizes ResNet-50. Err. means the average error rate (%) of all 15 corruptions, Avg. err. and Avg. mem means the average error rate (%) and the average memory (MB) of overall batch sizes, respectively. Mem. denotes total memory consumption, including model parameter sizes and activations. The lowest error is in bold, and the second lowest error is underlined.

Datasets	Method	Batch Size												Avg. err Avg. mem	
		128		64		32		16		8		4			
		Err.	Mem.	Err.	Mem.	Err.	Mem.	Err.	Mem.	Err.	Mem.	Err.	Mem.		
CIFAR10-C	Source	43.5	204.3	43.5	120.4	43.5	78.4	43.5	57.5	43.5	47.0	43.5	41.7	43.5	91.6
	EATA	18.7	1240.3	20.3	638.4	23.9	337.5	28.9	187.0	47.2	111.8	47.2	74.2	31.0	431.5
	Continual TENT	25.6	1240.3	38.1	638.4	46.5	337.5	62.2	187.0	78.7	111.8	86.4	74.2	56.3	431.5
	CoTTA	17.9	2939.1	18.7	1688.4	22.2	1063.1	34.5	750.4	59.3	594.1	79.0	515.9	38.6	1133.4
	SWA	17.7	2939.1	18.6	1688.4	21.7	1063.1	31.8	750.4	56.9	594.1	76.3	515.9	37.2	1133.4
	ECoTTA	19.6	747.2	21.8	397.0	22.3	221.8	39.8	134.3	46.7	90.5	54.2	68.6	34.1	276.6
	SAR	20.4	1240.3	20.7	638.4	21.4	337.5	22.9	187.0	32.6	111.8	75.7	74.2	32.3	431.5
	LAW	16.3	2647.3	17.5	1396.6	18.6	771.3	22.8	458.6	51.2	302.3	78.2	224.1	34.1	966.7
	FoCTTA (Ours)	16.7	356.0	17.3	197.9	18.9	118.9	21.6	79.4	27.1	59.7	35.7	49.8	22.9	143.6
CIFAR100-C	Source	46.8	35.8	46.8	19.0	46.8	10.6	46.8	6.4	46.8	4.4	46.8	3.3	46.8	13.3
	EATA	36.1	367.2	37.0	184.7	39.7	93.5	44.1	47.9	51.7	25.1	74.7	13.7	47.2	122.0
	Continual TENT	41.3	367.2	49.0	184.7	79.2	93.5	87.0	47.9	95.4	25.1	98.3	13.7	75.0	122.0
	CoTTA	38.1	783.6	39.6	405.3	43.4	216.2	51.6	121.6	71.4	74.3	91.3	50.7	55.9	275.3
	SWA	37.8	783.6	39.1	405.3	42.8	216.2	50.3	121.6	69.6	74.3	90.1	50.7	55.0	275.3
	ECoTTA	37.2	174.8	37.9	88.8	39.6	45.8	46.2	24.3	85.7	13.6	96.4	8.2	57.2	59.3
	SAR	35.5	367.2	36.2	184.7	40.2	93.5	68.7	47.9	94.1	25.1	98.3	13.7	62.2	122.0
	LAW	35.6	779.0	36.1	400.7	38.1	211.6	42.4	117.0	56.9	69.7	92.0	46.1	50.2	270.7
	FoCTTA (Ours)	34.3	88.4	34.7	45.9	35.8	24.7	38.7	14.1	44.5	8.8	73.6	6.1	43.6	31.3
ImageNet-C	Source	82.4	1053.2	82.4	539.4	82.4	282.5	82.4	154.0	82.4	89.8	82.4	57.7	82.4	362.8
	EATA	59.1	5780.3	60.8	2903.0	63.7	1464.4	68.9	745.0	79.9	385.4	86.4	205.5	69.8	1913.9
	Continual TENT	67.0	5780.3	67.5	2903.0	71.7	1464.4	91.7	745.0	97.4	385.4	99.3	205.5	82.4	1913.9
	CoTTA	65.9	11520.4	66.1	5913.5	67.3	3110.1	82.2	1708.3	96.5	1007.5	99.7	657.1	79.6	3986.2
	SWA	65.3	11520.4	65.8	5913.5	66.7	3110.1	81.4	1708.3	93.6	1007.5	99.4	657.1	78.7	3986.2
	ECoTTA	80.8	2540.2	89.7	1332.7	97.8	729.0	99.5	427.2	99.8	276.2	99.8	200.8	94.6	917.7
	SAR	61.9	5780.3	62.4	2903.0	63.8	1464.4	76.7	745.0	80.4	385.4	85.2	205.5	71.7	1913.9
	LAW	60.7	11316.0	61.4	5709.1	62.9	2905.9	74.4	1503.9	94.2	803.1	98.9	452.7	75.4	3531.1
	FoCTTA (Ours)	61.4	1598.4	62.8	814.8	65.1	423.0	68.1	227.2	77.0	129.2	83.0	80.3	69.6	545.5

Table 5: **Ablation study on data augmentation type.** From left to right one augmentation type is added at a time.

augmentation type	color jitter	+horizontal flip	+gaussian blur	+invert
Avg err.(%)	36.4	36.2	35.9	35.8

Table 6: **Average inference time per domain on the CIFAR10-C dataset using WideResNet-28 with a batch size of 32.** Also, we show the average error rates (%) overall 15 corruptions.

Method	Adaptation time (s)	Error rate (%)
Source	5.6	43.5
Continual TENT	33.2	46.5
CoTTA	1854.4	22.2
SWA	1650.6	21.7
SAR	40.7	21.4
EATA	32.1	23.9
LAW	60.2	18.6
ECotTA	65.1	22.3
FoCoTTA (Ours)	16.4	18.9

reliable samples for model optimization, further reducing adaptation time.

Integrate BN layer optimization. In Table 7, we integrated FoCTTA with the BN layer optimization method MECTA (Hong et al. 2023). Encouragingly, their com-

bined application further reduced FoCTTA’s error rate from 18.9% to 17.1%. This not only validates the effectiveness of FoCTTA but also expands its applicability.

Comparison with fine-tuning methods. We conducted a comparison between FoCTTA and various methods that directly fine-tune the adaptation model on the CIFAR10-C dataset. The evaluation utilized the WideResNet-28 model, employing the Adam optimizer with a learning rate of 0.001 and a batch size of 32. To ensure a fair comparison, all methods utilized identical hyperparameters throughout the adaptation process. From Table 8, we found that fine-tuning all convolutional layers yields the poorest performance, whereas fine-tuning the BN layer results in suboptimal performance. Notably, the exclusive fine-tuning of the BN layer, incorporating tracking statistics during adaptation, leads to a lower error rate. Compared to all methods, our FoCTTA consistently attains the lowest error rate.

Visualization. In Fig. 4, we visualize the discriminative capabilities of different methods on the same batch sample in CIFAR10-C. From the figure, we observe that our FoCTTA, like other methods, exhibits discriminative abilities. This further substantiates the effectiveness of FoCTTA.

Table 7: **Integrate FoCTTA with the BN layer optimization method MECTA.** The evaluation using WideResNet-28 on the CIFAR10-C dataset with a batch size of 32, demonstrates improved performance.

Method	t →															Avg. err
	Gaus.	Shot	Impu.	Defo.	Glas.	Moti.	Zoom	Snow	Fros.	Fog	Brig.	Cont.	Elas.	Pixe.	Jpeg	
EATA	24.9	21.2	31.4	18.6	35.4	21.8	19.5	21.9	20.9	22.6	15.8	20.3	30.0	26.1	28.0	23.9
+ MECTA	25.8	20.1	29.9	12.6	31.0	13.7	11.0	16.1	15.1	13.3	8.3	11.0	20.0	15.7	20.8	17.6
TENT	26.3	25.8	38.5	32.2	48.2	40.2	43.7	47.5	45.7	48.1	46.2	62.6	61.9	63.9	66.7	46.5
+ MECTA	25.6	20.7	28.9	13.2	29.7	14.1	12.0	16.8	15.4	15.2	8.7	13.5	19.5	15.5	20.3	17.9
FoCoTTA (Ours)	23.8	22.3	30.1	13.7	32.2	14.4	12.6	16.4	16.5	13.8	8.6	16.5	24.1	16.7	21.1	18.9
+ MECTA	22.6	19.1	25.2	13.0	32.1	13.7	10.9	14.9	15.2	12.8	7.8	12.8	21.7	15.0	19.6	17.1

Table 8: **We conduct a comparison between FoCTTA and various methods that directly fine-tune the adaptation model on the CIFAR10-C dataset.** The evaluation utilized the WideResNet-28 model with a batch size of 32, and the results demonstrate a substantial improvement in performance with our approach.

Method	t →															Avg. err
	Gaus.	Shot	Impu.	Defo.	Glas.	Moti.	Zoom	Snow	Fros.	Fog	Brig.	Cont.	Elas.	Pixe.	Jpeg	
FC-Tune	28.9	27.2	37.3	14.0	36.1	15.3	13.5	18.7	18.8	16.6	9.2	14.2	25.2	21.0	28.2	21.6
Conv-Tune	90.1	89.1	90.4	89.9	90.0	87.6	89.3	89.6	89.5	89.9	89.5	91.5	90.0	89.2	89.4	89.7
BN-Tune	28.3	26.1	36.1	13.9	35.0	15.0	13.3	18.4	18.8	16.2	9.3	14.1	24.8	21.1	27.4	21.2
No-Adapt	72.3	65.7	72.9	46.9	54.3	34.8	42.0	25.1	41.3	26.0	9.3	46.7	26.6	58.5	30.3	43.5
FoCoTTA (Ours)	23.8	22.3	30.1	13.7	32.2	14.4	12.6	16.4	16.5	13.8	8.6	16.5	24.1	16.7	21.1	18.9

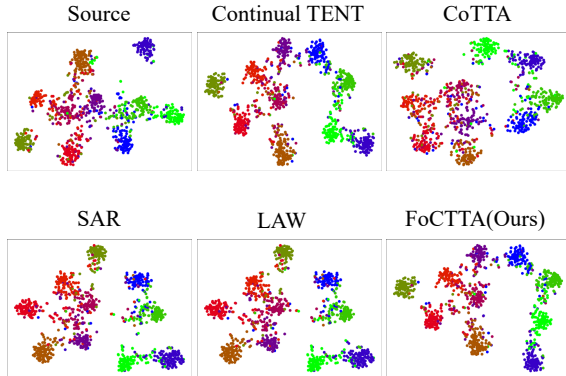


Figure 4: **Visualization of the discriminative power of the sample features of different methods on CIFAR10-C.** Colors represent sample classes.

Table 9: **Avg err.(%) with different values of λ .**

λ	0.1	0.5	0.9	1.0	1.2	1.5
Avg err.(%)	36.0	35.9	35.9	35.8	36.0	36.1

Ablation Study

In the following experiments, if not specified, we use CIFAR100-C and robustly pre-trained WideResNet-40.

Necessity of Each Design. Table 3 demonstrates the influence of removing individual designs in FoCTTA on its performance. The results show a significant performance decline when any FoCTTA design is removed, highlighting the crucial role of each design in achieving exceptional performance. Particularly, the choice of the adaptation-critical layer is vital for FoCTTA, and its absence leads to performance collapse.

Table 10: **Avg err.(%) with different values of α .**

α	0.03	0.05	0.08	0.1	0.15	0.20
Avg err.(%)	37.9	36.8	36.0	35.8	35.8	36.1

Influence of λ and α : Table 9 and Table 10 show the effect of λ and α on the error rate of FoCTTA, respectively. Here, λ represents the weight of the regularization term. α represents the number of adaptation-critical layers selected for optimization. We choose the setting that achieves the best performance, with $\lambda = 1.0$ and $\alpha = 0.1$ as default values.

Influence of the data augmentation type: We use data augmentation in the warm-up training phase to simulate domain shifts. Table 5 demonstrates the influence of data augmentation types on FoCTTA, revealing its robustness. By using default settings, we choose color jittering and inverting, achieving the best performance.

Conclusion

In this paper, our focus is on addressing the memory efficiency issues during the adaptation of CTTA. To this end, we propose FoCTTA, a new low-memory CTTA strategy. Rather than blindly update all BN layers, we identify and adapt a few drift-sensitive representation layers. The shift from BN to representation layers eliminates the need for large batch sizes. Furthermore, by updating adaptation-critical layers only, FoCTTA avoids storing excessive activations. This approach improves memory efficiency and maintains adaptation effectiveness, as confirmed by evaluations across various models and datasets.

References

- Arazo, E.; Ortego, D.; Albert, P.; O'Connor, N. E.; and McGuinness, K. 2020. Pseudo-labeling and confirmation bias in deep semi-supervised learning. In *2020 International Joint Conference on Neural Networks (IJCNN)*, 1–8. IEEE.
- Boudiaf, M.; Mueller, R.; Ben Ayed, I.; and Bertinetto, L. 2022. Parameter-free online test-time adaptation. In *Proceedings of the IEEE/CVF Conference on Computer Vision and Pattern Recognition*, 8344–8353.
- Cai, H.; Gan, C.; Zhu, L.; and Han, S. 2020. Tinytl: Reduce memory, not parameters for efficient on-device learning. *Advances in Neural Information Processing Systems*, 33: 11285–11297.
- Chen, Y.; Niu, S.; Xu, S.; Song, H.; Wang, Y.; and Tan, M. 2024. Towards Robust and Efficient Cloud-Edge Elastic Model Adaptation via Selective Entropy Distillation. *arXiv preprint arXiv:2402.17316*.
- Cheng, H.; Zhang, M.; and Shi, J. Q. 2023. A survey on deep neural network pruning-taxonomy, comparison, analysis, and recommendations. *arXiv preprint arXiv:2308.06767*.
- Choi, S.; Yang, S.; Choi, S.; and Yun, S. 2022. Improving test-time adaptation via shift-agnostic weight regularization and nearest source prototypes. In *European Conference on Computer Vision*, 440–458. Springer.
- Croce, F.; Andriushchenko, M.; Schwag, V.; Debenedetti, E.; Flammarion, N.; Chiang, M.; Mittal, P.; and Hein, M. 2020. Robustbench: a standardized adversarial robustness benchmark. *arXiv preprint arXiv:2010.09670*.
- Deng, J.; Dong, W.; Socher, R.; Li, L.-J.; Li, K.; and Fei-Fei, L. 2009. Imagenet: A large-scale hierarchical image database. In *2009 IEEE conference on computer vision and pattern recognition*, 248–255. Ieee.
- Gan, Y.; Bai, Y.; Lou, Y.; Ma, X.; Zhang, R.; Shi, N.; and Luo, L. 2023. Decorate the newcomers: Visual domain prompt for continual test time adaptation. In *Proceedings of the AAAI Conference on Artificial Intelligence*, 7595–7603.
- Gao, Z.; Zhang, X.-Y.; and Liu, C.-L. 2024. Unified Entropy Optimization for Open-Set Test-Time Adaptation. In *Proceedings of the IEEE/CVF Conference on Computer Vision and Pattern Recognition (CVPR)*, 23975–23984.
- Gong, T.; Kim, Y.; Lee, T.; Chottananurak, S.; and Lee, S.-J. 2023. SoTTA: Robust Test-Time Adaptation on Noisy Data Streams. *arXiv preprint arXiv:2310.10074*.
- Han, S.; Pool, J.; Tran, J.; and Dally, W. 2015. Learning both weights and connections for efficient neural network. *Advances in neural information processing systems*, 28.
- He, K.; Zhang, X.; Ren, S.; and Sun, J. 2016. Deep residual learning for image recognition. In *Proceedings of the IEEE conference on computer vision and pattern recognition*, 770–778.
- Hendrycks, D.; and Dietterich, T. 2019. Benchmarking neural network robustness to common corruptions and perturbations. *arXiv preprint arXiv:1903.12261*.
- Hong, J.; Lyu, L.; Zhou, J.; and Spranger, M. 2023. Mecta: Memory-economic continual test-time model adaptation. In *2023 International Conference on Learning Representations*.
- Jung, S.; Lee, J.; Kim, N.; Shaban, A.; Boots, B.; and Choo, J. 2023. Cafa: Class-aware feature alignment for test-time adaptation. In *Proceedings of the IEEE/CVF International Conference on Computer Vision*, 19060–19071.
- Krizhevsky, A. 2009. Learning Multiple Layers of Features from Tiny Images. *Master's thesis, University of Tront*.
- Lee, J.; Das, D.; Choo, J.; and Choi, S. 2023. Towards open-set test-time adaptation utilizing the wisdom of crowds in entropy minimization. In *Proceedings of the IEEE/CVF International Conference on Computer Vision*, 16380–16389.
- Lee, N.; Ajanthan, T.; and Torr, P. H. 2018. Snip: Single-shot network pruning based on connection sensitivity. *arXiv preprint arXiv:1810.02340*.
- Li, H.; Kadav, A.; Durdanovic, I.; Samet, H.; and Graf, H. P. 2016. Pruning filters for efficient convnets. *arXiv preprint arXiv:1608.08710*.
- Liang, J.; Hu, D.; and Feng, J. 2020. Do we really need to access the source data? source hypothesis transfer for unsupervised domain adaptation. In *International conference on machine learning*, 6028–6039. PMLR.
- Lim, H.; Kim, B.; Choo, J.; and Choi, S. 2022. TTN: A Domain-Shift Aware Batch Normalization in Test-Time Adaptation. In *The Eleventh International Conference on Learning Representations*.
- Lim, H.; Kim, B.; Choo, J.; and Choi, S. 2023. TTN: A domain-shift aware batch normalization in test-time adaptation. *arXiv preprint arXiv:2302.05155*.
- Lin, J.; Chen, W.-M.; Lin, Y.; Gan, C.; Han, S.; et al. 2020. Mcunet: Tiny deep learning on iot devices. *Advances in Neural Information Processing Systems*, 33: 11711–11722.
- Liu, Y.; Kothari, P.; Van Delft, B.; Bellot-Gurlet, B.; Moridan, T.; and Alahi, A. 2021. Ttt++: When does self-supervised test-time training fail or thrive? *Advances in Neural Information Processing Systems*, 34: 21808–21820.
- Liu, Z.; Li, J.; Shen, Z.; Huang, G.; Yan, S.; and Zhang, C. 2017. Learning efficient convolutional networks through network slimming. In *Proceedings of the IEEE international conference on computer vision*, 2736–2744.
- Ma, Y.; Chen, Y.; Yu, H.; Gu, Y.; Wen, S.; and Guo, S. 2023. Letting Go of Self-Domain Awareness: Multi-Source Domain-Adversarial Generalization via Dynamic Domain-Weighted Contrastive Transfer Learning. In *ECAI 2023-European Conference on Artificial Intelligence*, 1664–1671.
- Molchanov, P.; Tyree, S.; Karras, T.; Aila, T.; and Kautz, J. 2016. Pruning convolutional neural networks for resource efficient inference. *arXiv preprint arXiv:1611.06440*.
- Montesuma, E. F.; Mboula, F. M. N.; and Souloumiac, A. 2023. Multi-source domain adaptation through dataset dictionary learning in wasserstein space. In *ECAI 2023-European Conference on Artificial Intelligence*, volume 372, 1739–1746.
- Niu, S.; Wu, J.; Zhang, Y.; Chen, Y.; Zheng, S.; Zhao, P.; and Tan, M. 2022. Efficient test-time model adaptation without

forgetting. In *International conference on machine learning*, 16888–16905. PMLR.

Niu, S.; Wu, J.; Zhang, Y.; Wen, Z.; Chen, Y.; Zhao, P.; and Tan, M. 2023. Towards stable test-time adaptation in dynamic wild world. *arXiv preprint arXiv:2302.12400*.

Park, J.; Kim, J.; Kwon, H.; Yoon, I.; and Sohn, K. 2024. Layer-wise auto-weighting for non-stationary test-time adaptation. In *Proceedings of the IEEE/CVF Winter Conference on Applications of Computer Vision*, 1414–1423.

Paszke, A.; Gross, S.; Massa, F.; Lerer, A.; Bradbury, J.; Chanan, G.; Killeen, T.; Lin, Z.; Gimelshein, N.; Antiga, L.; et al. 2019. Pytorch: An imperative style, high-performance deep learning library. *Advances in neural information processing systems*, 32.

Song, J.; Lee, J.; Kweon, I. S.; and Choi, S. 2023. EcoTTA: Memory-Efficient Continual Test-Time Adaptation via Self-Distilled Regularization. In *Proceedings of the IEEE/CVF Conference on Computer Vision and Pattern Recognition (CVPR)*, 11920–11929.

Storkey, A.; et al. 2009. When training and test sets are different: characterizing learning transfer. *Dataset shift in machine learning*, 30(3-28): 6.

Tarvainen, A.; and Valpola, H. 2017. Mean teachers are better role models: Weight-averaged consistency targets improve semi-supervised deep learning results. *Advances in neural information processing systems*, 30.

Wang, D.; Shelhamer, E.; Liu, S.; Olshausen, B.; and Darrell, T. 2020. Tent: Fully Test-Time Adaptation by Entropy Minimization. In *International Conference on Learning Representations*.

Wang, Q.; Fink, O.; Van Gool, L.; and Dai, D. 2022. Continual test-time domain adaptation. In *Proceedings of the IEEE/CVF Conference on Computer Vision and Pattern Recognition*, 7201–7211.

Wang, Y.; Hong, J.; Cheraghian, A.; Rahman, S.; Ahmedt-Aristizabal, D.; Petersson, L.; and Harandi, M. 2024. Continual test-time domain adaptation via dynamic sample selection. In *Proceedings of the IEEE/CVF Winter Conference on Applications of Computer Vision*, 1701–1710.

Yang, X.; Gu, Y.; Wei, K.; and Deng, C. 2023. Exploring safety supervision for continual test-time domain adaptation. In *Proceedings of the Thirty-Second International Joint Conference on Artificial Intelligence*, 1649–1657.

You, F.; Li, J.; and Zhao, Z. 2021. Test-time batch statistics calibration for covariate shift. *arXiv preprint arXiv:2110.04065*.

Yuan, L.; Xie, B.; and Li, S. 2023. Robust test-time adaptation in dynamic scenarios. In *Proceedings of the IEEE/CVF Conference on Computer Vision and Pattern Recognition*, 15922–15932.

Zagoruyko, S.; and Komodakis, N. 2016. Wide residual networks. *arXiv preprint arXiv:1605.07146*.